

Effect of Buffer Layers on Electrical, Optical and Structural Properties of AlGaIn/GaN Heterostructures Grown on Si

Chin-An CHANG*, Shao-Tang LIEN, Chen-Han LIU, Chaun-Feng SHIH, Nie-Chuan CHEN, Pen-Hsiu CHANG, Hien-Chiu PENG, Tze-Yu TANG, Wei-Chieh LIEN, Yu-Hsiang WU, Kun-Ta WU¹, Ji-Wei CHEN¹, Chi-Te LIANG¹, Yang-Fang CHEN¹, Tong-Uan LU² and Tai-Yuan LIN²

Institute of Electro-Optical Engineering, Chang Gung University, Tao-Yuan, Taiwan, Republic of China

¹*Department of Physics, National Taiwan University, Taipei, Taiwan, Republic of China*

²*Institute of Optoelectronic Sciences, National Taiwan Ocean University, Keelung, Taiwan, Republic of China*

(Received October 12, 2005; accepted December 16, 2005; published online April 7, 2006)

AlGaIn/GaN heterostructures with different buffer layers were grown on Si substrates by metal-organic vapor phase epitaxy (MOVPE). The electrical property of the two-dimensional electron gas (2DEG) formed at the AlGaIn/GaN interface was correlated with both the optical and structural quality of the GaN layer involved. A combination of two sets of high-temperature and low-temperature AlN and an ultrashort exposure to SiH₄ showed the best-grown GaN, followed by a similar buffer layer without the SiH₄ exposure, and a graded AlGaIn buffer layer only. The enhancements in both electron mobility and 2DEG density were also accompanied by a reduced donor–acceptor pair (DAP) emission and a reduced dislocation density in the top GaN grown. [DOI: 10.1143/JJAP.45.2516]

KEYWORDS: AlGaIn/GaN, 2DEG, buffer layer, defects, Si substrate, MOVPE

The AlGaIn/GaN interface has been an intensive subject for both fundamental and applied research. The formation of a two-dimensional electron gas (2DEG) at the AlGaIn/GaN interface has been attributed to the large piezoelectric field present.¹⁾ Such a field is commonly noted when a strained AlGaIn is grown on a completely relaxed GaN layer. The large piezoelectric field thus present allows the injection of charges from the AlGaIn into the GaN layer without the need of heavy doping of the former. The source of the charges is believed to include surface defects in the AlGaIn layer, with carrier densities as high as 10^{13} cm^{-2} being commonly observed in such heterostructures.^{2,3)} Upon cooling, depending on the structures grown on sapphire, the electron mobility reaches $10,000 \text{ cm}^2 \text{ V}^{-1} \text{ s}^{-1}$ or higher, and levels off below about 100 K.^{4,5)} Using GaN substrate, an electron mobility exceeding $100,000 \text{ cm}^2 \text{ V}^{-1} \text{ s}^{-1}$ at 4 K and lower temperatures has been reported for the AlGaIn/GaN heterostructures grown by molecular beam epitaxy (MBE).^{6,7)}

In this Communication, we report the electrical, optical and structural study of AlGaIn/GaN heterostructures grown on Si substrate. The growth of nitrides on Si is known to be difficult due to the large thermal stress present. Extensive effort has been devoted to reduce this problem, including the use of AlN intermediate layers.^{8–11)} We have recently reported the growth of nitride light-emitting diodes (LEDs) on Si.¹²⁾ Both blue and green LEDs were made with an output power of 0.7 mW, likely among the best reported. Using phosphors for the blue LED made, a white emission was also achieved. We are here extending the nitride-on-Si work to other electronic devices to explore the combined effects of lattice and thermal mismatch. Different buffer layers were tested for reducing the defect propagation into the critical AlGaIn/GaN interface where the 2DEG channel was formed.

All the structures reported here were grown by metal-organic vapor phase epitaxy (MOVPE) using an Aixtron 200/4 RF-S system. Most samples were grown on (111)Si substrate, with some grown on (0001) sapphire substrate for comparison. Using Si, a low-temperature AlN nucleation

layer was first grown at 525 °C. This was followed by a different sequence of layers as shown below. Except otherwise indicated, all the GaN and AlGaIn layers were grown at 1050 °C. The flow rates for the Al and Ga sources were 20 sccm for TMA and 10–25 sccm for TMG, respectively. The ammonia flow rate was 600–1600 sccm. The analyses included Hall measurement, photoluminescence (PL), X-ray diffraction (XRD), scanning electron microscopy (SEM), atomic force microscopy (AFM), Raman spectroscopy, and cross-sectional transmission electron microscopy (XTEM).

Three structures were compared using the Si substrate. Sample A: p-Si/LT-AlN (2.5 nm)/graded AlGaIn (150 nm)/GaN (187.5 nm)/Al_{0.15}Ga_{0.85}N (30 nm); Sample B: p-Si/LT-AlN (12 nm)/HT-AlN (12 nm)/GaN (350 nm)/LT-AlN (12 nm)/HT-AlN (12 nm)/GaN (400 nm)/Al_{0.15}Ga_{0.85}N (30 nm); Sample C: p-Si/LT-AlN (12 nm)/HT-AlN (12 nm)/ultrathin Si_xN_y/GaN (350 nm)/LT-AlN (12 nm)/HT-AlN (12 nm)/GaN (400 nm)/Al_{0.15}Ga_{0.85}N (30 nm). LT and HT AlN were for the AlN layers grown at 620 °C (low temperature) and 1050 °C (high temperature), respectively. The ultrathin SiN layer of Sample C was grown at 1050 °C, with a 30 s exposure to SiH₄ at 3333×10^{-7} sccm and NH₃ at 600 sccm. Several samples were grown on sapphire. One, Sample D, with the structure of sapphire/LT-GaN buffer (25 nm)/GaN (1.5 μm)/Al_{0.15}Ga_{0.85}N (30 nm) was used to compare with those grown on Si.

Table I lists the electrical, optical, Raman, XRD, PL, and TEM measurements of the four structures listed above. Comparing with the GaN film grown on GaN substrate, where a Raman E₂ (high) of 568 cm^{-1} was reported,¹³⁾ all the samples here showed reduced vibration frequencies. This indicated a tensile strain in the top GaN layer that was in direct contact with the top AlGaIn layer. Samples A, B, and C showed the order of increasing 2DEG carrier density and electron mobility, and decreasing full-width at half-maximum (FWHM) for both XRD rocking curves and PL linewidths. The electrical measurements over the temperatures of 10–300 K are shown in Fig. 1 for Samples B, C, and D. No low-temperature measurement was carried out for Sample A due to its low electron mobility at room temper-

*E-mail address: cac@mail.ggu.edu.tw

Table I. Comparison of samples grown on Si and sapphire: Raman frequency, charge density, electron mobility, FWHM of XRD rocking curve and PL emission, and dislocation density.

Sample	substrate	E_2 (cm^{-1})	n_s ($10^{13}/\text{cm}^2$)	μ ($\text{cm}^2/\text{V s}$)	XRD-FWHM PL-FWHM dislocation		
					(arcsec)	(meV)	(10^9 cm^{-2})
	Comment	RT	RT	RT	GaN(0002)	10 K	Top GaN
A	Si(111)	564.3	1.02	140	597	16.4	3.2
B	Si(111)	564.4	1.18	570	502	15.6	0.9
C	Si(111)	565.1	1.60	610	495	14.5	0.6
D	Al_2O_3	567.8	1.93	650	296	4.6	N/A

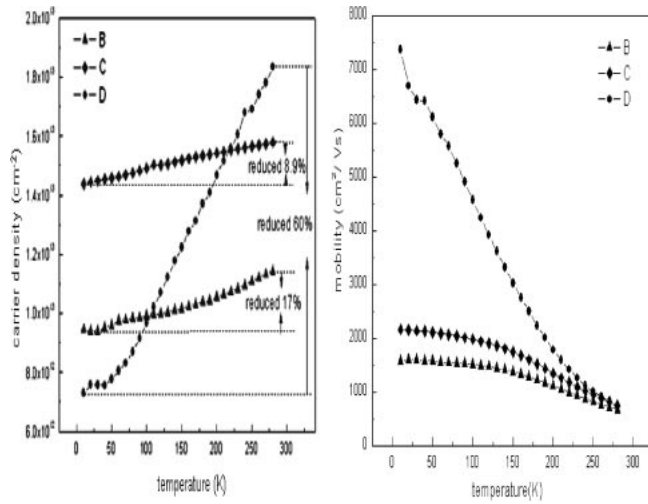


Fig. 1. Charge density and electron mobility of Samples B and C grown on Si, and Sample D grown on sapphire.

ature. An increased mobility at low temperatures was noted for all three samples, with that of Sample D being the highest. In fact, the mobility of Sample D was still rising at 10 K while those grown on Si leveled off at such temperatures.

The quality of the 2DEG formed closely depended on the GaN layer present. It is thus necessary to assess the GaN layers involved in the different structures. The photoluminescence measurement, shown in Fig. 2, provided some information in this regard. In addition to the band-edge emission of GaN, additional peaks at lower energies were noted for the samples grown on Si. These are labeled as donor-acceptor pair (DAP) for the donor-acceptor pair, and their phonon replicas.^{14,15} The intensity of the DAP and phonon replica peaks decreased from Samples A to B to C. In contrast, these peaks were completely absent for Sample D grown on sapphire. The DAP emission of GaN was generally attributed to defects involving N vacancies and N interstitials.^{14,15} The decreasing DAP emission was accompanied by the increasing carrier density and electron mobility, with a similar narrowing of the FWHM for both XRD and PL. These all indicated a likely correlation between the electrical property of the 2DEG formed and the GaN layer involved.

The growth of nitride films on Si involves large lattice and thermal mismatches. The effect of different buffer layers on the generation and propagation of defects is shown in Fig. 3. All the individual layers were shown with the estimated dislocation density indicated. The dislocation density was an

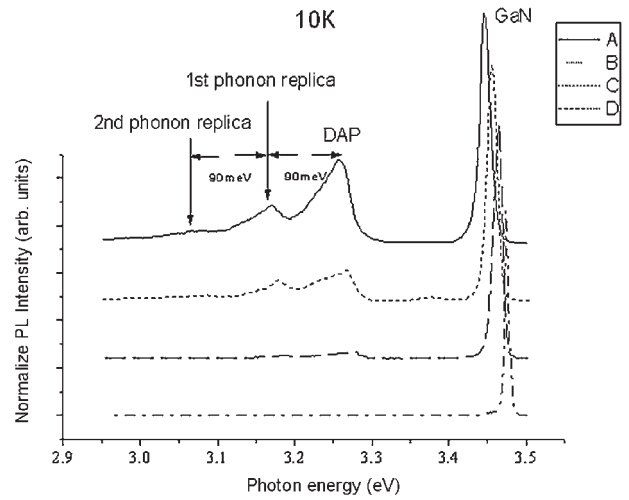


Fig. 2. Photoluminescence measurement of GaN band-edge emission, donor-acceptor pair (DAP) and its phonon replicas of Samples A, B, and C, grown on Si, and Sample D grown on sapphire.

estimated average from different areas of each sample. A decreasing dislocation density in the top GaN layer, also listed in Table I, was noted from Samples A to B to C. This was consistent with the order of improving electrical and optical properties for such samples. No data was shown for the sample grown on sapphire due to the much thicker GaN layer present.

We have compared AlGaIn/GaN heterostructures on Si with different buffer layers. Due to the large thermal stress between Si and nitride layers, cracking has been widely observed.⁸⁻¹² The use of only a low-temperature (LT) AlN layer resulted in a nonsmooth growth surface that could be smoothed out by a subsequent high-temperature (HT) AlN layer. A double LT-AlN and HT-AlN combination for Sample B was more effective than a single grading AlGaIn layer for Sample A. This could involve a number of factors. The continual grading of the AlGaIn layer in Sample A was aimed at reducing the lattice mismatch from the AlN/Si interface to the final GaN layer. The graded AlGaIn layer may have partially achieved the purpose, but could not stop the defect generated at the Si/AlN interface due to the large mismatch there. Furthermore, the AlGaIn grading layer alone could not help reduce the thermal stress present. This is consistent with the cracking of Sample A as observed from the SEM analysis. Sample B contained two sets of LT-AlN/HT-AlN layers and showed an effective reduction in cracking. The buffer layers also contributed to a reduced propagation of dislocation from the Si interface into the final GaN layer. As Fig. 3 indicates, the dislocation densities of

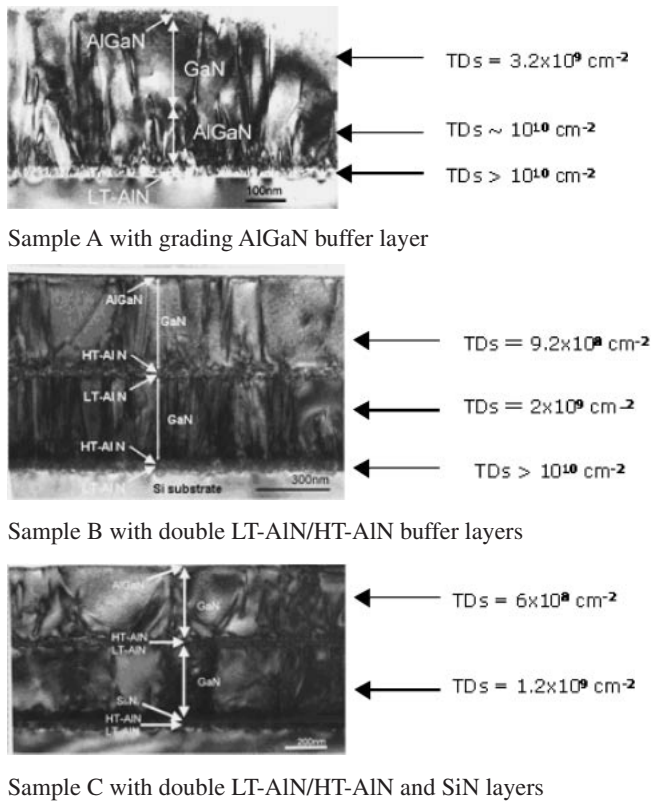


Fig. 3. Cross-sectional transmission electron micrograph of defect generation and propagation of Samples A, B, and C grown on Si.

the first and second GaN layers were 2×10^9 and $9.2 \times 10^8 \text{ cm}^{-2}$, respectively. A comparison of the first GaN layer of Sample B with the GaN layer of Sample A indicated that the first LT-AlN/HT-AlN buffer layer also contributed to the reduced defect propagation from the Si interface. The presence of the second LT-AlN/HT-AlN buffer layer further helped the growth of a second GaN layer with a lower defect density. The use of double LT-AlN/HT-AlN buffer layers thus played dual factors of reducing both the cracking and defect propagation.

A similar effect was observed for Sample C which had both the double LT-AlN/HT-AlN buffer layers and an ultrathin SiN layer after the first LT-AlN/HT-AlN buffer layers. Using high-resolution TEM, we could not detect any amorphous SiN layer. Instead, the lattice showed a continuing single-crystalline structure across the whole film of Sample C. Apparently, the ultrathin SiN layer, if formed, did not affect the crystalline growth of subsequent nitride layers.¹⁶⁾ Yet, it helped reduce the dislocation as compared with that of Sample B. This is interesting in that Sample C also showed improved electrical and optical properties over Sample B as described above.

The TEM analysis has confirmed the dependence of the top GaN on the buffer layers used. It also indicated the roles of the AlN layers in reducing the cracking due to thermal stress. The quality of the top GaN layer plays a dominant role in the properties of the 2DEG channel formed with the surface AlGaIn layer. An improved epitaxy of the GaN layer also led to an improved growth of the AlGaIn layer that, in turn, helped the 2DEG formed.

All the samples grown on Si in this study showed properties inferior to those of a simple AlGaIn/GaN

structure grown on sapphire. The Raman analysis, for example, provided information regarding the strain in the top GaN layer. As indicated in Table I, the E_2 (high) energy differed among the samples analyzed. Comparing with the E_2 (high) value of 568 cm^{-1} for the GaN film grown on a GaN substrate,¹³⁾ the reduced numbers in Table I indicated an increasing tensile strain in the samples reported, being the largest for Sample A, and smallest for Sample C. The tensile strain of Sample D was smaller than all the samples grown on Si. The observed tensile stress was consistent with a previous report on the GaN layer grown on Si using the AlN buffer layers.¹⁷⁾

The large reduction in charge density upon cooling for Sample D is interesting. The reported 2DEG for the AlGaIn/GaN heterostructures often showed a large rise in mobility followed by a leveling upon cooling, with a rather constant charge density at low temperatures.²⁻⁷⁾ Sample D showed both a large reduction in charge density and a rising electron mobility at low temperatures. Cooling could either freeze out the charges due to the defects present or result in a reduced charge transfer from the AlGaIn layer. The likely role of the defect was likely to cause a reduced mobility also, contrary to the results of measurement here. The reduced charge transfer, on the other hand, would reduce the impurity scattering due to less ionized impurity in the AlGaIn layer, resulting in increasing electron mobility. Further analysis is needed to fully understand the mechanism involved.

- 1) H. Morkoc, A. D. Carlo and R. Cingolani: in *Low-Dimensional Nitride Semiconductors*, ed. B. Gil (Oxford University Press, New York, 2002) p. 341.
- 2) J. P. Ibbetson, P. T. Fini, K. D. Ness, S. P. DenBaars, J. S. Speck and U. K. Mishra: *Appl. Phys. Lett.* **77** (2000) 250.
- 3) S. Heikman, S. Keller, Y. Wu, J. S. Speck, S. P. DenBaars and U. K. Mishra: *J. Appl. Phys.* **93** (2003) 10114.
- 4) I. P. Smorchkova, C. R. Elsass, J. P. Ibbetson, R. Vetury, B. Heying, P. Fini, E. Haus, S. P. DenBaars, J. S. Speck and U. K. Mishra: *J. Appl. Phys.* **86** (1999) 4520.
- 5) M. Miyoshi, H. Ishikawa, T. Egawa, K. Asai, M. Mouri, T. Shibata, M. Tanaka and O. Oda: *Appl. Phys. Lett.* **85** (2004) 1710.
- 6) M. J. Manfra, K. W. Baldwin, A. M. Sergent, K. W. West, R. J. Molnar and J. Caissie: *Appl. Phys. Lett.* **85** (2004) 5394.
- 7) C. Skierbiszewski, K. Dybko, W. Knap, M. Siekacz, W. Krupczynski, G. Nowak, M. Bockowski, J. Lusakowski, Z. R. Wasilewski, D. Maude, T. Suski and S. Porowski: *Appl. Phys. Lett.* **86** (2005) 102106.
- 8) J. Baasking, A. Reiher, A. Dedgar, A. Diez and A. Krost: *Appl. Phys. Lett.* **81** (2002) 2722.
- 9) A. Dagar, M. Poschenrieder, J. Blasing, K. Fehse, A. Diwz and A. Krost: *Appl. Phys. Lett.* **80** (2002) 3670.
- 10) B. Zhang, T. Egawa, H. Ishikawa, Y. Liu and T. Jimbo: *Jpn. J. Appl. Phys.* **42** (2003) L226.
- 11) T. Egawa, T. Moku, H. Ishikawa, K. Ohtsuka and T. Jimbo: *Jpn. J. Appl. Phys.* **41** (2002) L663.
- 12) C.-F. Shih, N.-C. Chen, C.-A. Chang and K.-S. Liu: *Jpn. J. Appl. Phys.* **44** (2005) L140.
- 13) H. Harima: *J. Phys.: Condens. Matter* **14** (2002) R967, and references therein.
- 14) D. C. Look, D. C. Reynolds, J. W. Hemsky, J. R. Sizelove, R. L. Jones and R. J. Molnar: *Phys. Rev. Lett.* **79** (1997) 2273.
- 15) G. B. Ren, D. J. Dewsnip, D. E. Lacklison, J. W. Orton, T. S. Cheng and C. T. Foxon: *Mater. Sci. Eng. B* **43** (1997) 242.
- 16) K. Pakula, R. Bozek, J. M. Baranowski, J. Jasinski and Z. Liliental-Weber: *J. Cryst. Growth* **267** (2004) 1.
- 17) B. H. Bairamov, O. Gurdal, A. Botchkarev, H. Morkoc, G. Irmer and J. Monecke: *Phys. Rev. B* **60** (1999) 16741.